Synthesis and Direct Visualization of Block Copolymers Composed of Different Macromolecular Architectures

Jeffrey Pyun,[†,‡] Chuanbing Tang,[§] Tomasz Kowalewski,[§] Jean M. J. Fréchet,[*,‡] and Craig J. Hawker[*,†]

IBM Almaden Research Center, 650 Harry Road, San Jose, California 95120, Department of Chemistry, University of California, Berkeley, California 94720, and Department of Chemistry, Carnegie Mellon University, 4400 Fifth Avenue, Pittsburgh, Pennsylvania 15213

Received December 20, 2004

ABSTRACT: A novel approach toward the synthesis of block copolymers composed of architecturally different components, in this case, a nanoparticle covalently attached to a single linear coil is presented. By a synergistic combination of controlled radical polymerization, convergent dendrimer synthesis, and benzocyclobutene (BCB) cross-linking chemistry, strategies for the preparation of a variety of nanoparticle−coil copolymers were developed. Atomic force microscopy (AFM) was used to confirm the formation of architecturally differentiated block copolymers and enabled visualization of individual nanoparticles and their linear chain components for unambiguous characterization of the nanoparticle−coil structures. This confirmed the synthesis of the targeted nanostructure and revealed the dramatic effect that changes in macromolecular architecture can have on the morphology and assembly of these hybrid nanoparticle systems.

Introduction

The synthesis of novel polymeric materials is an evolving field of research with the preparation of macromolecules possessing precise structures coupled to improved properties being an area of particular interest. In this respect, synthetic polymers currently lag behind biological systems, as mimicry of the intricate topology, 3-dimensional structure, and functionality of biological polymers remains a difficult challenge. Naturally occurring polymers, namely, enzymes and proteins, often incorporate different architectures (i.e., globular, linear) into a single macromolecule enabling the creation of discrete nanoenvironments for catalysis and self-assembly.[1a,b] Recent developments in polymer therapeutics have seen the launching of several highly successful drugs with mixed globular-linear architecture in which a globular protein is attached to a synthetic linear polymer such as poly(ethylene glycol).[1c] In these systems the synthetic linear-globular assembly shows vast performance enhancements over the natural globular protein on its own.

Despite these advances, biological mimicry in the world of synthetic polymers is still in its infancy and it is important to develop our abilities to prepare and characterize macromolecular isomers and large architecturally defined assemblies through nanoscale control of both the structure and the properties of the synthetic constructs.[2] The ability to tune properties of bulk materials has been extensively pursued by directed self-assembly of block copolymers, in both solution and in the solid state,[2a−f] to form well-defined phase separated structures, or nano-objects.[2g−i] Recent advances in synthetic polymer chemistry have enabled the preparation of a much wider variety of well-defined di- and multiblock copolymers[3] and these systems demonstrate that the morphology and properties of polymeric materials can be dictated by composition, molar mass and architecture of the copolymer segments. Of these structural aspects, architecture is the most poorly studied, yet it has the potential to be an extremely powerful tool for controlling material properties.

To this end, hybrid materials composed of dendritic and linear segments are an interesting class of block copolymer that combine components of very different architecture and composition into a single macromolecule.[4] Although still relatively unexplored, hybrid dendron−coil copolymers have been shown to possess unusual solid-state morphologies[5] and have generated interest as potential carriers for targeted drug delivery.[6] The synthesis of dendron−coil copolymers possessing dendritic, or branched, segments of high molar mass however still remains a difficult challenge due to the multistep synthesis required to prepare large dendrimers, limiting the molecular weight of the dendron fragment to less than 5000 g/mol.

In related studies, developments in living anionic polymerization have enabled the synthesis of asymmetric stars containing branched and linear segments in the same macromolecules.[7] These routes afford well-defined block copolymers of precise architecture and composition, though inherent difficulties associated with sensitivity toward various functional groups have limited the application of this approach.

To overcome issues of molecular size and availability of materials, an accelerated route to hybrid block copolymers composed of nanoparticles and linear polymers has recently been demonstrated using controlled radical polymerization[3d,g,h] in which the 3-dimensional, dendron-like block segments have much higher molecular weights (e.g., MW greater than 50 000 g/mol).[8] Herein, we report the synergistic use of dendrimer synthesis and controlled radical polymerization for the preparation of functional linear macromolecular architectures, which serve as useful precursors to hybrid nanoparticle−coil copolymers. By the combination of

* Corresponding author. E-mail: hawker@almaden.ibm.com.
† IBM Almaden Research Center.
‡ University of California.
§ Carnegie Mellon University.

10.1021/ma047375f CCC: $30.25
Published on Web 03/01/2005

Scheme 1. Synthesis of Nanoparticle−Coil Copolymer (2) from Linear Diblock Copolymer Precursor (1)

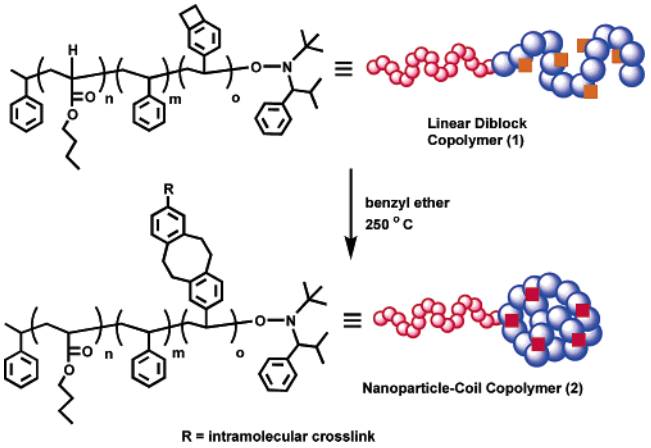

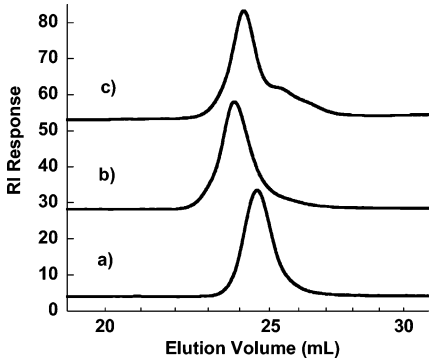

Figure 1. SEC plots of (a) pBA macroinitiator (M_n = 56 000 g/mol; M_w/M_n = 1.18), (b) pBA-*b*-p(S-*r*-BCB) diblock copolymer precursor **1** (M_n = 89 000 g/mol; M_w/M_n = 1.41), and (c) particle−coil copolymer (**2**) ($M_{n\ apparent}$ = 55 000 g/mol; M_w/M_n = 1.56) prepared from thermal induced cross-linking of **1**.

these controlled polymerizations with the benzocyclobutene (BCB) cross-linking process,[8] well-defined molecular objects possessing a polymeric nanoparticle and a single linear chain were prepared.

The imaging of these molecular objects with molecular resolution using atomic force microscopy (AFM) is an extremely powerful technique for confirming the preparation and structure of complex polymeric nanostructures.[9] Recent success in AFM imaging of various polymeric structures has been reported with dendrimers,[10] graft and dendrigraft copolymers,[11] dendronized polymers,[12] and molecular polymer brushes.[13]

Compared to other techniques, the real strength of AFM is in directly visualizing the shape and structure of single macromolecules or molecular assemblies and when applied to complex polymer architectures have permitted the unprecedented characterization of these systems. For molecular brushes with both linear and starlike architectures, Sheiko and Matyjaszewski were able to determine and quantify arm length, defect structures, and molecular organization by high-resolution AFM.[14] Cylindrical macromolecular architectures such as dendronized linear polymers have also been visualized by both the groups of Möller and Percec[15] and their adsorption and organization on highly orientated substrates examined. In perhaps the most far reaching application of molecular visualization and polymer architecture, Schlüter has employed AFM, to not only visualize these 3-dimensional macromolecules, but to manipulate the position of single molecules.[16] By using photochemically active chain end functionalized dendronized linear polymers, an elementary step toward molecular nanoconstruction was taken in subsequently covalently connecting two individual polymer chains.

By combining new synthetic strategies for nanoparticle-linear macromolecules with structural analysis by AFM, the preparation and visualization of novel hybrid architecture is reported.

Results and Discussion

A. Nanoparticle—Coil Copolymers from Linear Diblock Copolymers. The initial approach for the preparation of nanoparticle−coil diblock copolymers involved the synthesis of linear diblock copolymers, followed by selective intramolecular cross-linking of the linear block containing pBCB groups (Scheme 1).[17] Nanoparticle−coil copolymers composed of a linear poly(*n*-butyl acrylate) (pBA) and a polystyrenic nanoparticle were anticipated to yield optimal structures for AFM visualization as previous reports on pBA containing polymer brushes have demonstrated that the spreading of pBA segments on polar surfaces facilitated the imaging of individual macromolecules with single chain resolution.[12] Furthermore, the enhanced rigidity of the intramolecularly cross-linked nanoparticle was expected to impart both sharp height and phase contrast relative to the linear segment during visualization of the nanoparticle−coil structures. Linear copolymers of poly(*n*-butyl acrylate)-*block*-poly(styrene-*random*-(4-vinylbenzocyclobutene) (pBA-*b*-p(S-*r*-BCB)) were therefore prepared by sequential polymerization of *n*-butyl acrylate (BA) followed by a mixture of styrene (Sty) and 4-vinylbenzocyclobutene (BCB).[17] Copolymers possessing radii of gyration (R_g) greater than 5 nm were targeted to facilitate characterization of the particle−coil copolymer using AFM.

In the first step of the synthesis, a pBA macroinitiator (M_n = 50 000; M_w/M_n = 1.18) was prepared by bulk polymerization of BA (7 M) at 125 °C in the presence of the alkoxyamine, 2,2,5-trimethyl-3-(1-phenoxyethyl)-4-phenyl-3-azahexane (7×10^{-3} M) and the corresponding free nitroxide (5 mol % relative to alkoxyamine), reaching a conversion of 54% in 20 h. Chain-extension of the formed pBA macroinitiator was then performed in solution with Sty/BCB (4:1 molar feed ratio, in 50 vol % *o*-xylene) at 125 °C, where monomer conversions of 60% Sty and 59% BCB were obtained after 18 h. Characterization of the crude polymerization mixture using size exclusion chromatography (SEC) and ^{1}H NMR confirmed efficient blocking to the pBA segment as higher molar mass (M_n = 89 000; M_w/M_n = 1.41, Figure 1) and incorporation of p(S-*r*-BCB) (45 mol % pBA, 45 mol % pS, 10 mol % pBCB measured from ^{1}H NMR).

Hybrid nanoparticle−coil copolymer **2** was then prepared by the slow addition of the pBA-*b*-p(S-*r*-BCB) linear copolymer (**1**) to a benzyl ether solution at 250 °C (Scheme 1). Thermally induced intramolecular cross-linking of p(S-*r*-BCB) segments yielded the target copolymer (**2**), possessing a polystyrenic nanoparticle and a single linear coil of pBA. SEC confirmed a decrease in apparent molar mass and hydrodynamic volume consistent with nanoparticle formation (M_n = 55 000; M_w/M_n = 1.56) due to intramolecular cross-linking and chain collapse (Figure 1c). ^{1}H NMR confirmed intramolecular cross-linking of pBCB groups, by the loss of methylene protons from the pBCB groups at

Scheme 2. Limitations of Controlled Radical Polymerization Approach in the Synthesis of Nanoparticle−Coil Copolymer (2) from Linear Diblock Precursor (1)

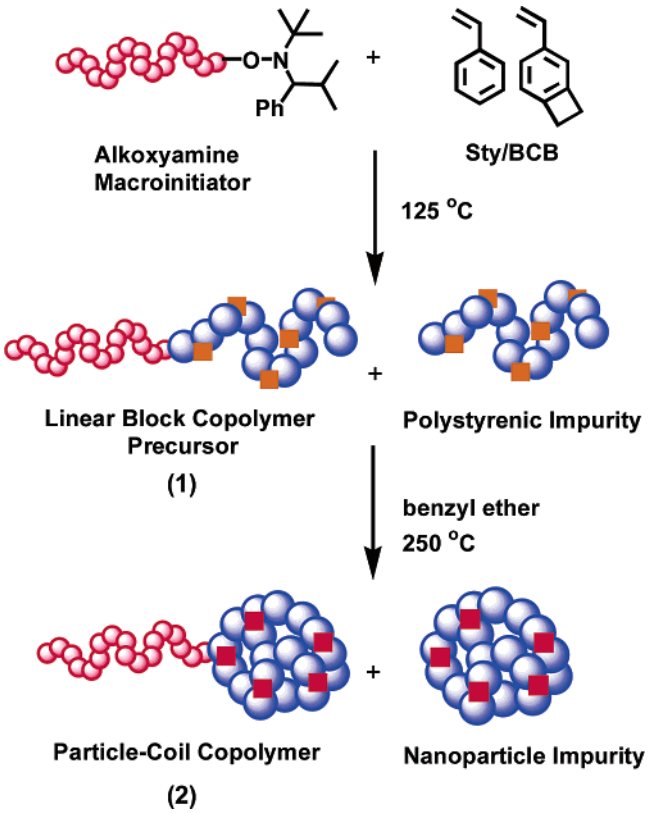

$\delta = 3.0$ and the appearance of resonances for cyclooctyl groups at $\delta = 2.6-2.8$ which are the primary product of the cross-linking reaction.[8]

The fidelity of the series of reactions resulting in the hybrid nanoparticle-linear structure was questioned by SEC which showed a lower molar mass shoulder in the chromatogram of nanoparticle−coil copolymer **2** prepared from pBA-*b*-p(S-*r*-BCB) precursor **1**. This was shown to be nanoparticles formed from p(S-*r*-BCB) contaminants and characterized as homopolymer p(S-*r*-BCB) impurities formed during the chain extension of the pBA macroinitaitor from thermal self-initiation of styrenic monomers (Scheme 2). The presence of the p(S-*r*-BCB) impurities was not evident in the SEC chromatograms of the crude product (Figure 1b) due to coincidental overlap of the pBA-*b*-p(S-*r*-BCB) block copolymer and p(S-*r*-BCB) contaminant, as well as, the polydispersity of the crude mixture. However, after addition to benzyl ether at 250 °C, the presence of both nanoparticle−coil copolymers from pBA-*b*-p(S-*r*-BCB) and nanoparticle impurities derived from p(S-*r*-BCB) contaminants could now be resolved due to the greater relative decrease in hydrodynamic volume for the homopolymer contaminant on collapse when compared to the block copolymer. This ability to distinguish the homopolymer contamination by chemistry in situations where it is difficult using one-dimensional SEC and ^{1}H NMR is an interesting feature of different macromolecular architectures.

By rigorous fractional precipitation and preparatory GPC, small amounts of pure diblock, **1**, and hybrid nanoparticle, **2**, could be obtained for AFM and DSC analysis. Differential scanning calorimetry (DSC), before and after thermal treatment at 250 °C, further confirmed the synthesis of hybrid linear nanoparticle diblock copolymers. For the linear pBA-*b*-p(S-*r*-BCB) (**1**)-two thermal transitions were observed corresponding to the glass transitions (T_g) of pBA ($T_g = -45$ °C) and p(S-*r*-BCB) ($T_g = 110$ °C). Nanoparticle−coil copolymers (**2**) also exhibited two transitions assigned to the T_g of pBA (−45 °C) and a transition at 55 °C attributed to the nanoparticle segment.[18]

B. Nanoparticle-Coil Copolymers from Dendritic Initiators. To overcome the difficulties in preparing hybrid nanoparticle−coil structures using linear diblock copolymers, an alternative strategy was designed using dendritic initiators to prepare asymmetric star copolymers containing pBCB groups, which could then be collapsed to give the desired products. It was envisaged that the star copolymer strategy would greatly facilitate the purification of these materials from homopolymer impurities. In this approach, poly(benzyl ether) (pBE) dendrons possessing latent initiator groups for atom transfer radical polymerization (ATRP) at the periphery and an alkoxyamine at the focal point were prepared with typical ATRP initiating groups, benzylic halides and α-haloesters, as the chain ends.[3g] This enables the preparation of an asymmetric star with multiple short arms of p(S-*r*-BCB) and a single long pBA chain. Subsequent intramolecular cross-linking of p(S-*r*-BCB) chains would give a nanoparticle−coil copolymer possessing a polystyrenic nanoparticle and a single pBA linear coil (Scheme 3). The use of a dendritic initiator circumvents many of the problems encountered using the linear diblock copolymer precursor. In particular, the functional dendritic initiator ensures high retention of initiating sites and allows reactions to be performed in an orthogonal fashion. Additionally, the use of ATRP to grow p(S-*r*-BCB) chains at lower temperatures sufficiently suppressed the contribution of thermal self-initiation and any chains that were prepared would be of a much lower molecular weight and therefore easily removed by precipitation.

Synthesis of Fourth Generation Dendritic Initiator. Because of difficulties in carrying α-haloester and benzyl bromide chain ends through a traditional convergent growth approach,[19] a protected Fréchet-type poly(benzyl ether) fourth generation dendron ((THP)$_{16}$-[G-4]) possessing 16-peripheral tetrahydropyranyl (THP) protecting groups and an alkoxyamine focal point was initially prepared.[20] The resulting hexadeca THP derivative, **3**, was then deprotected with para-toluenesulfonic acid to give the phenolic derivative, **4**, in greater than 95% conversion, however difficulties in purifying **4** resulted in a decreased yield of 54% after purification. Esterification of the terminal phenolic groups with 2-bromoisobutyryl bromide then yielded the multifunctional dendritic initiator **5** in 70% yield after purification by column chromatography.

Initially, the strategy to prepare hybrid nanoparticle−coil copolymers using dendritic initiator **5** involved copolymerization of styrene and 4-vinylbenzocyclobutene (BCB) under ATRP conditions from the peripheral 2-bromoisobutyrate groups, followed by nitroxide mediated polymerization of butyl acrylate (BA) from the focal point. However, ATRP experiments using the dendritic initiator **5** proved to be difficult due to the temperature sensitivity of the alkoxyamine. Previously reported conditions for the ATRP of styrenic monomers from multiple functional initiators employed high temperatures ($T = 90-130$ °C) with less reactive catalysts, such

Scheme 3. General Approach to Synthesize Nanoparticle−Coil Copolymers Using a Dendritic initiator

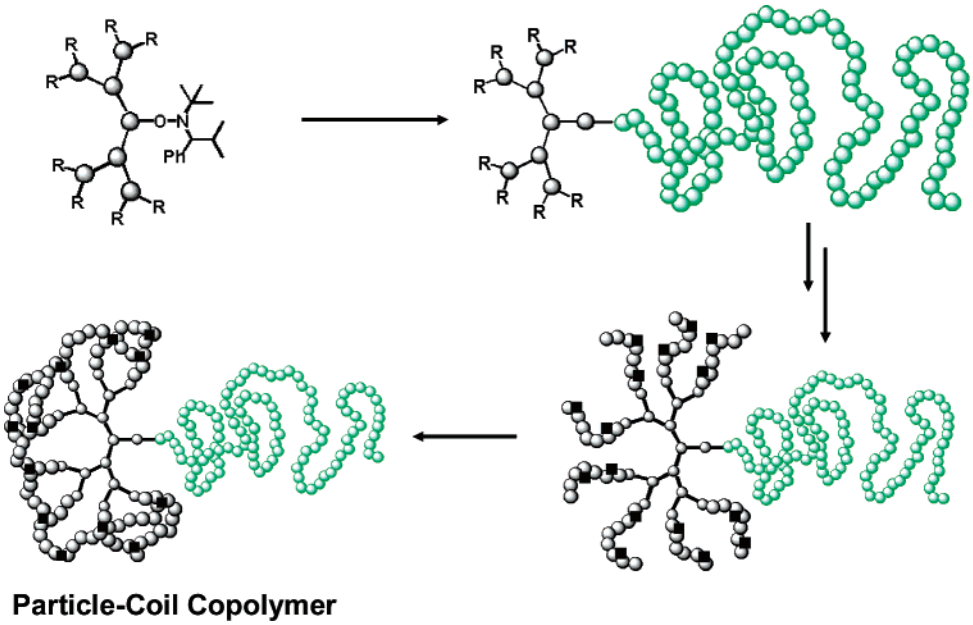

Scheme 4. Synthesis of Dendritic Initiator (5) Composed of Fourth Generation Fréchet-Type Dendron Containing 16 Initiation Sites for ATRP at the Periphery and a Single Alkoxyamine Focal Point[a]

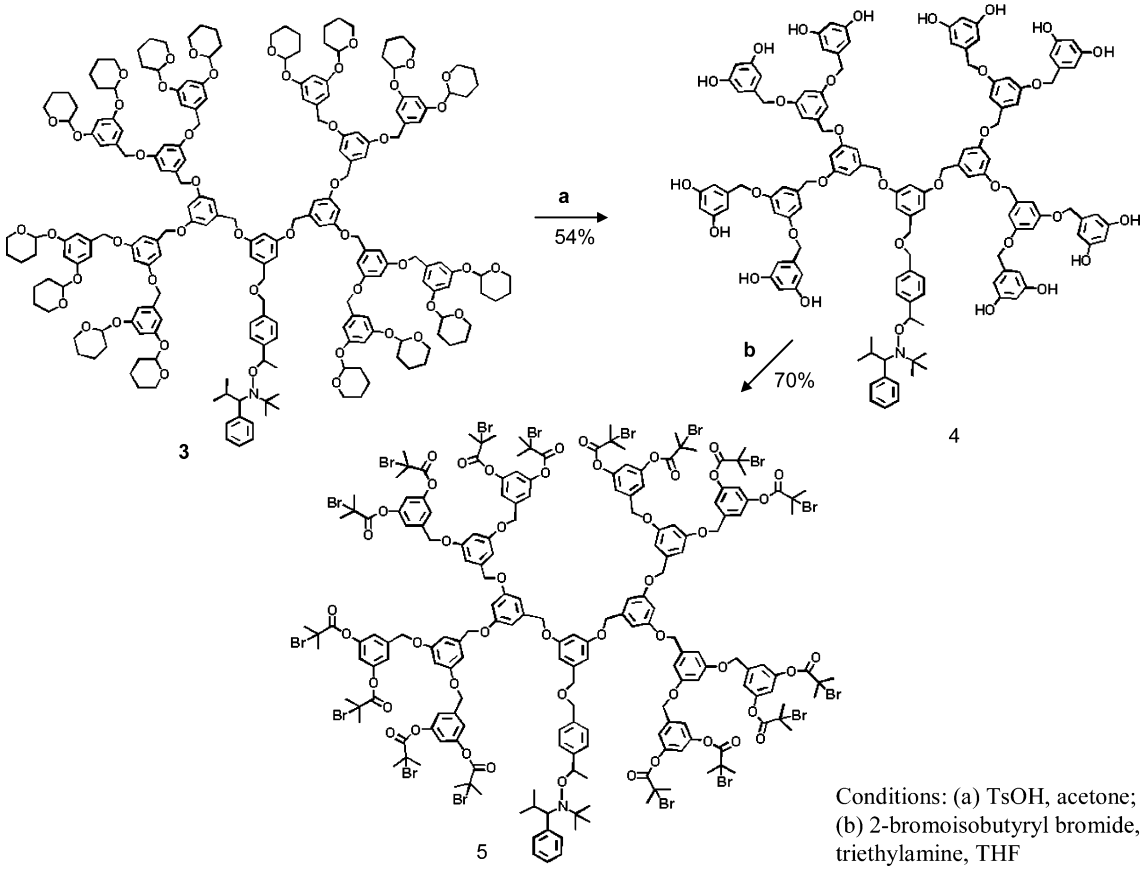

[a] Conditions: (a) TsOH, acetone; (b) 2-bromoisobutyryl bromide, triethylamine, THF.

as copper(I) bromide−bipyridine (Cu^IBr/bpy) based systems and at these temperatures significant homolysis of the alkoxyamine group would be expected.[21] Thus, initial attempts to grow p(S-*r*-BCB) arms from **5** utilized more reactive catalysts based on Cu^IBr and aliphatic amines at 60−70 °C.[22] However, only limited monomer conversions (<10%) and low yields of p(S-*r*-BCB) star copolymers were obtained. Polymerization of Sty/BCB from **5** with Cu^IBr/bpy based catalysts were also attempted at 90 °C but only low conversions (<5%) were reached after long reaction times (t > 24 h). Attempts to first perform the nitroxide mediated growth of the linear poly(butyl acrylate) chain before ATRP from the dendritic chain ends also proved to be difficult and numerous problems were encountered when bulk nitroxide mediated polymerizations of BA from the focal

Scheme 5. Synthesis of Dendritic Initiator (14) Using the Convergent Growth Approach[a]

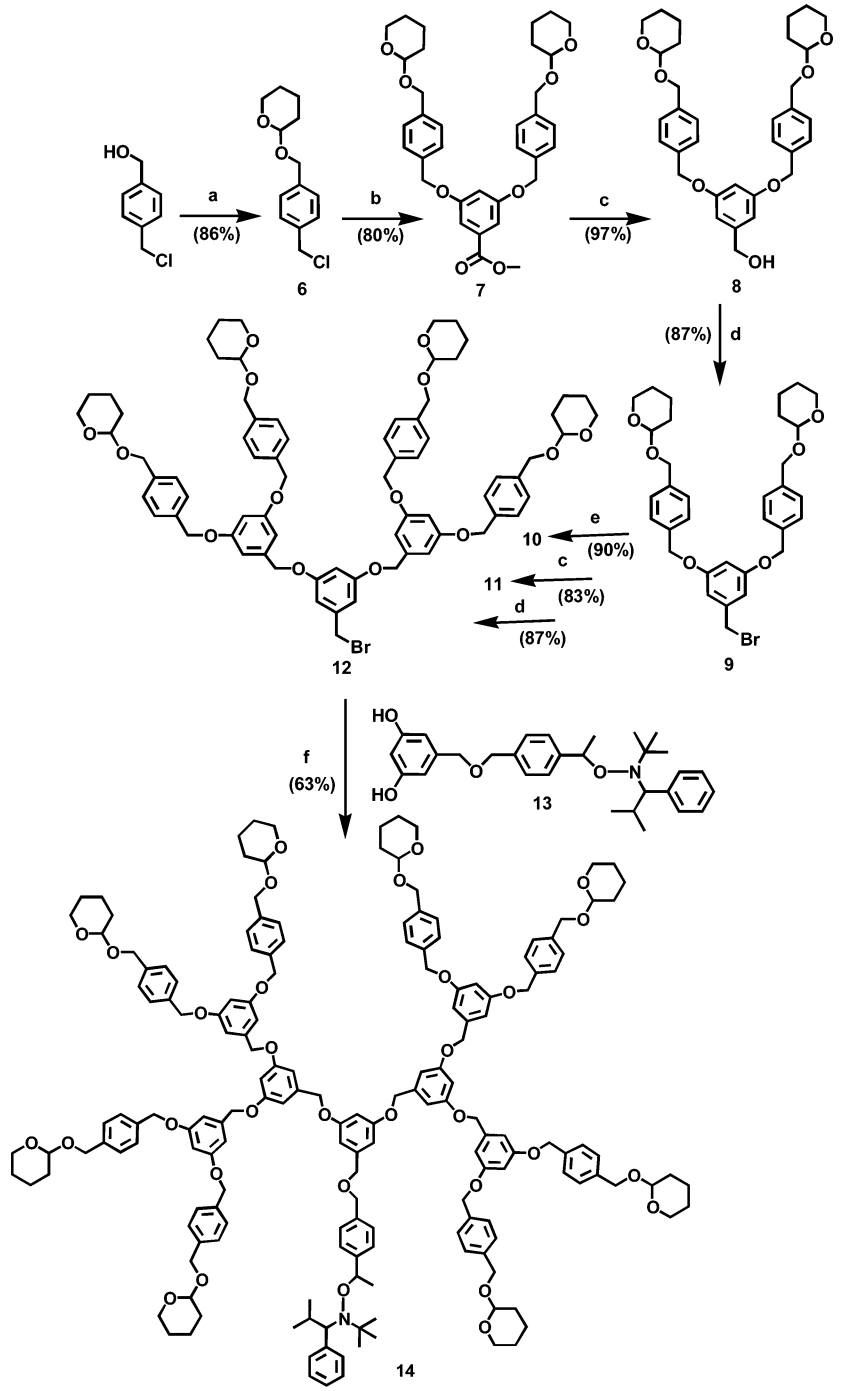

[a] Conditions: (a) 3,4-dihydro-2*H*-pyran, HCl(aq), CH_2Cl_2; (b) K_2CO_3, 18-crown-6, KI, 3,5-dihydroxybenzoate, acetone; (c) $LiAlH_4$, THF; (d) CBr_4, PPh_3, Hünig's base, THF; (e) K_2CO_3, 18-crown-6, 3,5-dihydroxybenzoate; (f) K_2CO_3, 18-crown-6, **13**, acetone.

point of **5** were attempted using standard conditions at 125 °C. Despite long reaction times, polymerization of BA was not observed, presumably due to chain transfer reactions of formed radicals with terminal alkyl halide groups of the dendrimer.

Synthesis of Third Generation Dendritic Initiator and Dendron-Coil Macroinitiator. In light of these difficulties, an alternate dendritic initiator was designed to allow the sequential polymerization of butyl acrylate followed by styrene/BCB using nitroxide mediated and ATRP polymerizations, respectively. A novel Frechet-type dendritic initiator was synthesized using the convergent approach replacing the peripheral THP protected phenolic groups from **3**−**5** with benzylic THP-protecting groups (Scheme 5). The use of a benzylic THP-protected dendrimer was particularly advantageous as the benzylic−THP groups were shown not to interfere with the nitroxide mediated process and could be converted to ATRP initiating groups in a single step. Additionally, third generation dendritic initiators were targeted, as larger dendrons yielded more compact stars, which required higher degrees of polymerization per arm to enable visualization by AFM. As a result, the reaction sequence was nitroxide mediated growth of pBA from the focal point, followed by deprotection/functionalization of the THP chain ends and growth by ATRP of the Sty/BCB arms from the dendron periphery. This revised strategy proved to be versatile as polymer-

Scheme 6. Synthesis of the Hybrid Particle−Coil Copolymer (18) from the Dendritic Initiator (14)[a]

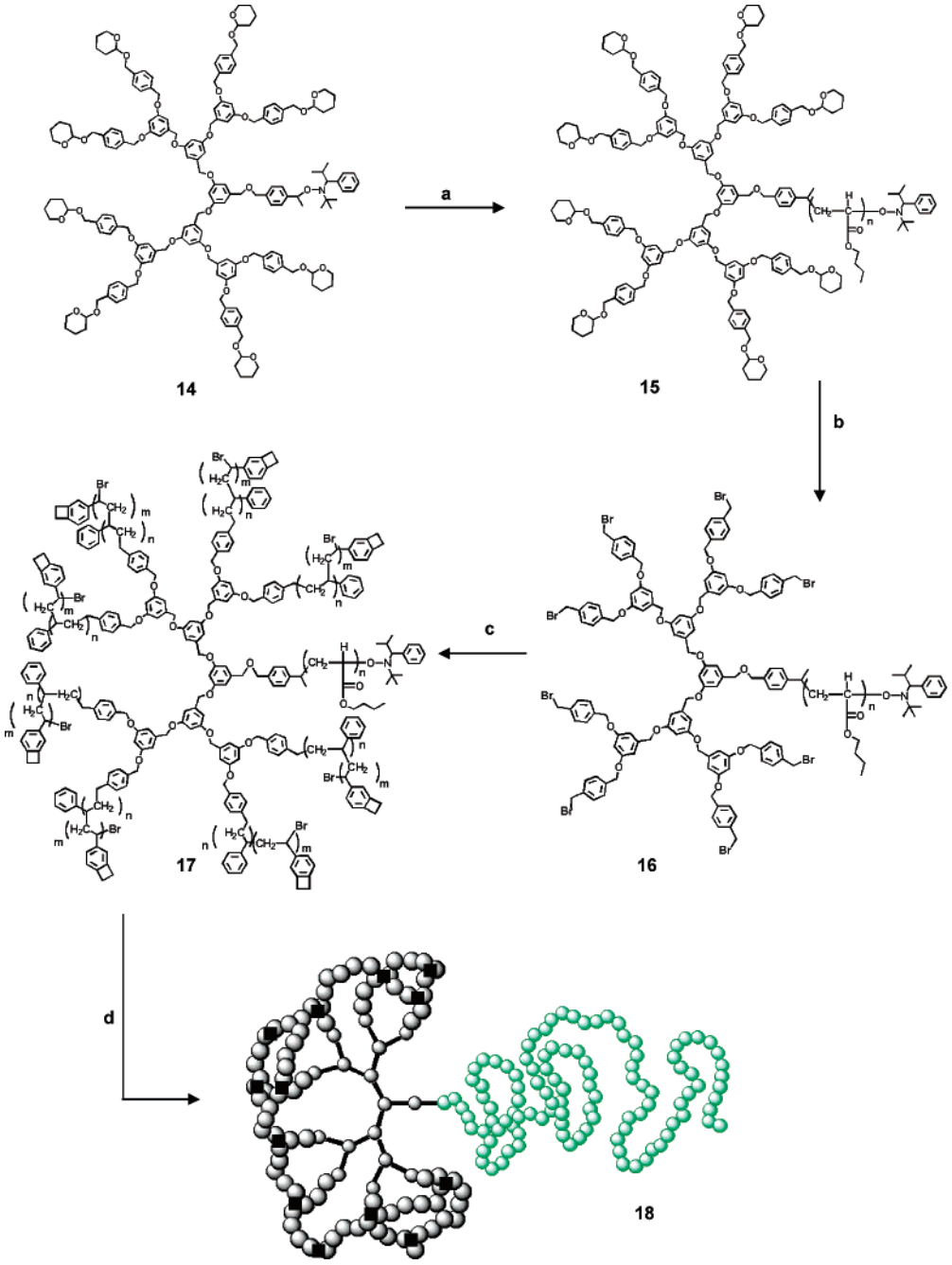

[a] Conditions: (a) *n*-butyl acrylate, 2,2,5-trimethyl-4-phenyl-3-azahexane-3-nitroxide, 125 °C; (b) Br_2, PPh_3, CH_2Cl_2, 0 °C; (c) styrene, 4-vinylbenzocyclobutene Cu(I)Br, 4,4′-dimethyl-2,2′-bipyridine, benzyl ether, 100 °C; (d) thermal cross-linking in benzyl ether at 250 °C.

izations from the focal point and the dendron periphery were performed in an orthogonal fashion, giving asymmetric stars and nanoparticle−coil copolymers of precise molar mass and low polydispersity.

The synthesis of the THP-protected dendrimers starting from the commercially available 4-(chloromethyl)-benzyl alcohol, which was protected by the acid-catalyzed addition of 3,4-dihydro-2*H*-pyran to give the benzylic-THP derivative, **6**. Alkylation of **6** with methyl 3,5 dihydroxybenzoate under phase transfer conditions afforded the first-generation ($(THPOCH_2)_2$-[G-1]-CO_2CH_3) methyl ester, **7**, in high yield. Subsequent reduction of **7** to **8** with lithium aluminum hydride (LAH), followed by bromination of the benzyl alcohol with CBr_4/PPh_3 in the presence of Hünig's base gave the benzyl bromide **9** ($(THPOCH_2)_2$-[G-1]-CH_2Br) in 87% yield. All attempts to brominate **8** under a variety of conditions in the absence of a base, such as Hünig's base, proved unsuccessful and resulted in significant deprotection of the THP protecting groups and decomposition. Generation growth was then accomplished by alkylation of **9** with methyl 3,5 dihydroxybenzoate to form **10**, reduction of the methyl ester with LAH ($(THPOCH_2)_4$-[G-2]-CH_2OH, **11**) and bromination of **11** gave the second generation dendritic bromide **12** ($(THPOCH_2)_4$-[G-2]-CH_2Br) in 92% yield. The final third generation dendritic initiator **14** was then obtained by coupling of **12** with the diphenolic alkoxyamine **13**[5a] and fully characterized by ^1H NMR, ^{13}C NMR, SEC and elemental analysis (Scheme 5).

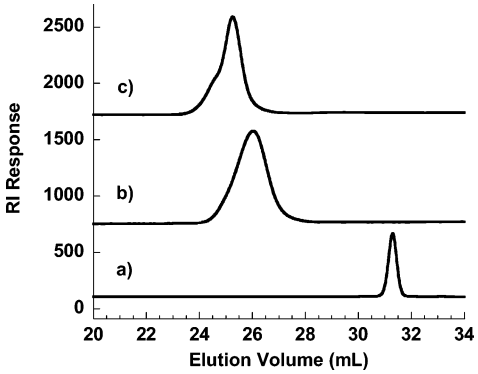

Figure 2. SEC plots of (a) dendritic initiator **14** (M_n = 2800 g/mol; M_w/M_n = 1.01), (b) [G-3]-*b*-pBA diblock copolymer **15** (M_n = 37 000 g/mol; M_w/M_n = 1.19), and (c) p(S-*r*-BCB)-*b*-[G-3]-*b*-pBA star copolymer **17** (M_n = 77 000 g/mol; M_w/M_n = 1.22).

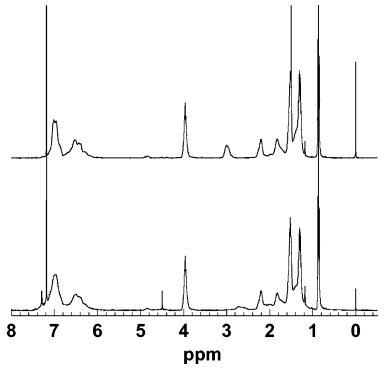

Figure 3. ^{1}H NMR spectra of p(S-*r*-BCB)-*b*-[G-3]-*b*-pBA star copolymer **17** (top) and nanoparticle−coil copolymer **18** (bottom) obtained after thermally induced cross-linking of p(S-*r*-BCB) arms.

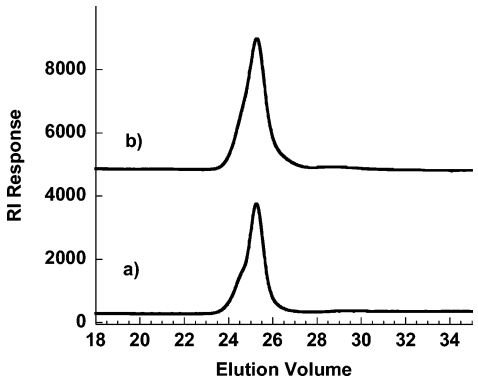

Figure 4. SEC plots of (a) p(S-*r*-BCB)-*b*-[G-3]-*b*-pBA star copolymer **17** (M_n = 77 000 g/mol; M_w/M_n = 1.22) and (b) nanoparticle−coil copolymer **18** ($M_{n\ apparent}$ = 62, 000 g/mol; M_w/M_n = 1.22) obtained after intramolecular cross-linking of **17**.

A hybrid dendron−coil block copolymer, [G-3]-*b*-pBA_{250} (**15**) (M_n = 37 000; M_w/M_n = 1.19) was then synthesized by the bulk nitroxide mediated polymerization of BA in the presence of dendritic initiator **14** and 5 mol % of free nitroxide. The molar mass and composition were determined from SEC (Figure 2) and ^{1}H NMR integration of the unique resonances for the dendron fragment and linear pBA chain and an initiation efficiency of greater than 90% was obtained for the polymerization of BA from the dendron focal point.[23] The copolymer could also be purified and trace amounts of residual initiator removed by filtration of the crude reaction mixture through a short plug of silica gel. This synthetic strategy afforded well-defined dendron−coil block copolymers possessing a single pBA chain bonded to a dendron with eight peripheral THP groups. The protected block copolymer **15** was converted in a single step to a dendron−coil macroinitiator for ATRP via bromination of peripheral benzylic−THP groups (Scheme 6). Conversion of the chain end THP groups to benzyl bromides in the presence of Br_2/PPh_3 proved to be quantitative, as determined from ^{1}H NMR, yielding the macroinitiator **16** in 90% yield after purification. This facile transformation of THP protected benzyl alcohols to ATRP initiating sites is a powerful synthetic technique and in this case enabled a wide range of styrenic and acrylate monomers to be polymerized from the dendron−coil macroinitiator to give asymmetric star copolymers.

Growth of the asymmetric star from the macroinitiator, **16**, involved ATRP polymerization of a mixture of styrene and 4-vinylbenzocyclobutene in the presence of a copper(I) bromide 4,4′-dimethyl-2,2′-bipyridine catalyst system at 100 °C. This afforded the $[p(S\text{-}r\text{-}BCB)_{45}]_8$-*b*-[G-3]-*b*-$pBA_{250}$ copolymer **17** (M_n = 77 000; M_w/M_n = 1.22) which contains eight p(S-*r*-BCB) arms and a single pBA linear coil connected by a poly(benzyl ether) dendritic fragment (Scheme 5). Comparison of SEC chromatograms from the dendritic initiator **14**, dendron−coil copolymer **15** and asymmetric star **17** showed a progressive increase in hydrodynamic size with each polymerization step while maintaining narrow molecular weight distributions with only minor amounts of chain−chain coupling being observed which leads to a small <5% higher molecular weight shoulder (Figure 2). When compared to the original sequential nitroxide mediated polymerization approach, where the linear diblock copolymer (**1**) contained p(S-*r*-BCB) contaminants of comparable size, requiring rigorous fractionation to isolate the pure pBA-*b*-p(S-*r*-BCB) block copolymer, the ATRP of Sty/BCB from the dendron coil macroinitiator was a significant improvement. As the p(S-*r*-BCB) arms were incorporated at lower temperatures, the formation of linear p(S-*r*-BCB) impurities was suppressed. Furthermore, any low molar mass linear p(S-*r*-BCB) contaminants that were formed could be easily removed from the larger asymmetric star **17** by simple precipitation. As expected, analysis of the $[p(S\text{-}r\text{-}BCB)_{45}]_8$-*b*-[G-3]-*b*-$pBA_{250}$ star copolymer **17** by DSC showed two thermal transitions at −39 °C and 93 °C which were assigned to the glass transitions (T_g) of pBA and p(S-*r*-BCB), respectively.

Synthesis of Nanoparticle—Coil Copolymers. The hybrid nanoparticle−coil copolymer, **18**, was then prepared from the star copolymer precursor **17** using similar conditions as for the synthesis of **2**. On the basis of the star copolymer structure, thermally induced intramolecular cross-linking of the p(S-*r*-BCB) arms results in formation of nanoparticle−coil copolymers consisting of a glassy PSt nanoparticle covalent attached to a single linear rubbery pBA coil. Comparison of the ^{1}H NMR spectra of star copolymer **17** and nanoparticle−coil copolymer **18** (Figure 3) verified consumption of pBCB (resonance at δ = 3.0) and the formation of cyclooctyl cross-links at δ = 2.6−2.8.[8] Additionally, resonances from the 3 different polymeric blocks; methylene protons from pBA at δ = 4.0, benzyl CH_2 units of the dendrimer at δ = 4.85, and aromatic protons at δ = 6−7.5 from pS were clearly resolved and unchanged after thermal treatment in benzyl ether at 250 °C. This confirms the presence of all block copolymer segments

Scheme 7. Synthesis of Nanoparticle−Coil Copolymer (22) with Inverted Composition[a]

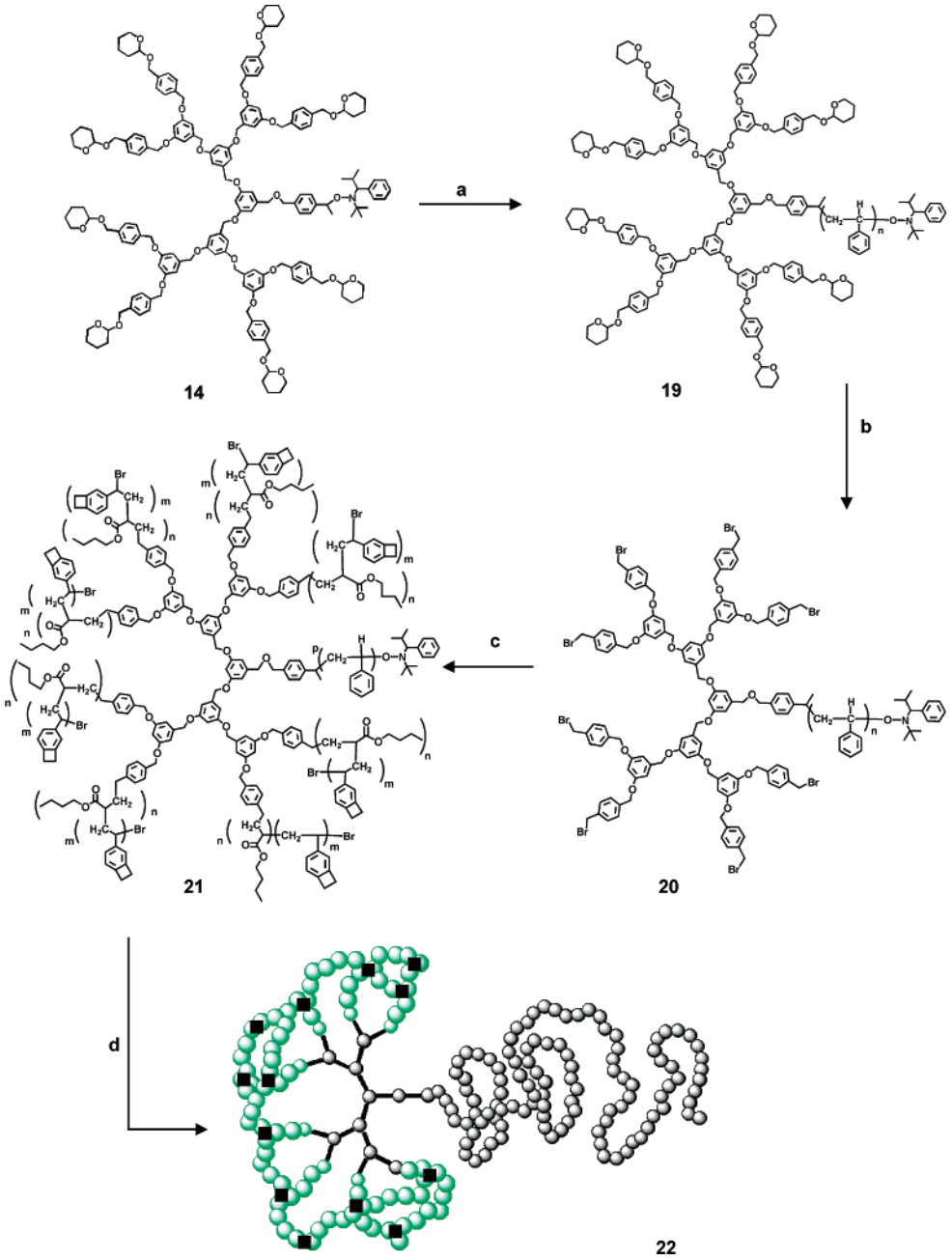

[a] A linear segment of PS is prepared in this system, along with a rubbery nanoparticle of pBA and pBCB. Conditions: (a) styrene, 125 °C; (b) Br_2, PPh_3, CH_2Cl_2, 0 °C; (c) *n*-butyl acrylate, 4-vinylbenzocyclobutene Cu^IBr, 4,4′di(5-nonyl)-2,2′-bipyridine, benzyl ether, 90 °C; (d) thermal cross-linking in benzyl ether at 250 °C.

in the final copolymer and the structural integrity of the hybrid system.

SEC further confirmed the synthesis of a well-defined nanoparticle−coil copolymer, as the chromatogram revealed that the final product possessed a relatively symmetrical molecular distribution and low polydispersity (M_w/M_n = 1.22, Figure 4). A slight decrease in apparent molar mass and hydrodynamic volume was observed due to intramolecular cross-linking of p(S-*r*-BCB) arms which is consistent with previous studies. However the higher solution density of star copolymer **17** relative to the linear diblock copolymer precursor did lead to only a minor change (ca. 20%) in hydrodynamic size being observed in the synthesis of **18**. In sharp contrast to the nanoparticle−coil copolymer **2**, derived from a linear diblock copolymer, lower molecular weight nanoparticle contaminants derived from p(S-*r*-BCB) impurities were not detected in the SEC of **18** which further validates the synthetic strategy

In an effort to further demonstrate the synthetic versatility of this system, the hybrid nanoparticle−coil copolymer **20** with an inverted composition relative to **18**, a glassy pS linear coil connected to a rubbery poly(butyl acrylate) nanoparticle was prepared (Scheme 7). Using a similar methodology as shown in Scheme 5, nitroxide mediated polymerization of styrene from the dendritic initiator, 14, gave the hybrid dendritic-linear copolymer, [G-3]-*b*-pS_{400} (M_n = 42 000; M_w/M_n = 1.14). Activation of the chain ends followed by ATRP of BA/BCB from the peripheral benzyl bromide groups gave the asymmetric star **21** with a composition of $[p(BA\text{-}r\text{-}BCB)_{60}]_8$-*b*-[G-3]-*b*-$pS_{400}$ (M_w/M_n = 84 000; M_w/M_n =

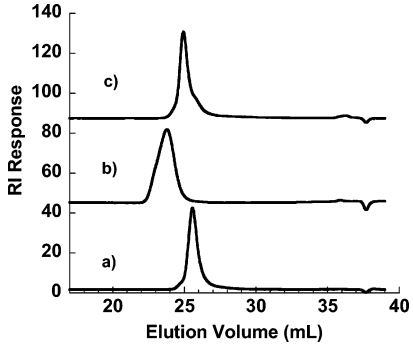

Figure 5. SEC plots of (a) [G-3]-*b*-pS macroinitiator (M_n = 42 000 g/mol; M_w/M_n = 1.18), (b) p(BA-*r*-BCB)-*b*-[G-3]-*b*-pS star copolymer **21** (M_n = 84 000 g/mol; M_w/M_n = 1.13), and (c) nanoparticle−coil copolymer **22** ($M_{n\ apparent}$ = 63 000 g/mol; M_w/M_n = 1.18) prepared from thermal induced cross-linking of **21**.

1.13). The addition of this star copolymer to a dilute benzyl ether solution at 250 °C yielded the final nanoparticle−coil copolymer **22** composed of a rubbery nanoparticle of cross-linked p(BA-*r*-BCB) bound to a single chain of glassy pS. Characterization of the nanoparticle−coil copolymer with an inverted composition was conducted using ^{1}H NMR, SEC and AFM. A stack SEC chromatogram of the pBE_{G3}-*b*-pS_{400} dendron−coil, [p(BA-*r*-BCB)$_{60}$)]$_8$-*b*-[G-3]-*b*-pS_{400} asymmetric star **21** and the inverted nanoparticle−coil copolymer **22** confirmed an increase in apparent molar mass after each polymerization step and a contraction of hydrodynamic size after the intramolecular cross-linking of p(BA-*r*-BCB) arms, while maintaining low polydispersities (M_w/M_n < 1.18) at each stage of the synthesis were maintained (Figure 5).

Visualization of Nanoparticle—Coil Copolymers. In previous studies,[11−13] architecturally distinct macromolecules were examined and visualized by AFM. The ability to prepare block copolymer structures consisting of more than one macromolecular architecture opens up the possibility of using AFM to distinguish individual blocks in a hybrid block copolymer visually and to confirm the structural evolution. To address this issue, purified nanoparticle−coil copolymers, **2**, obtained

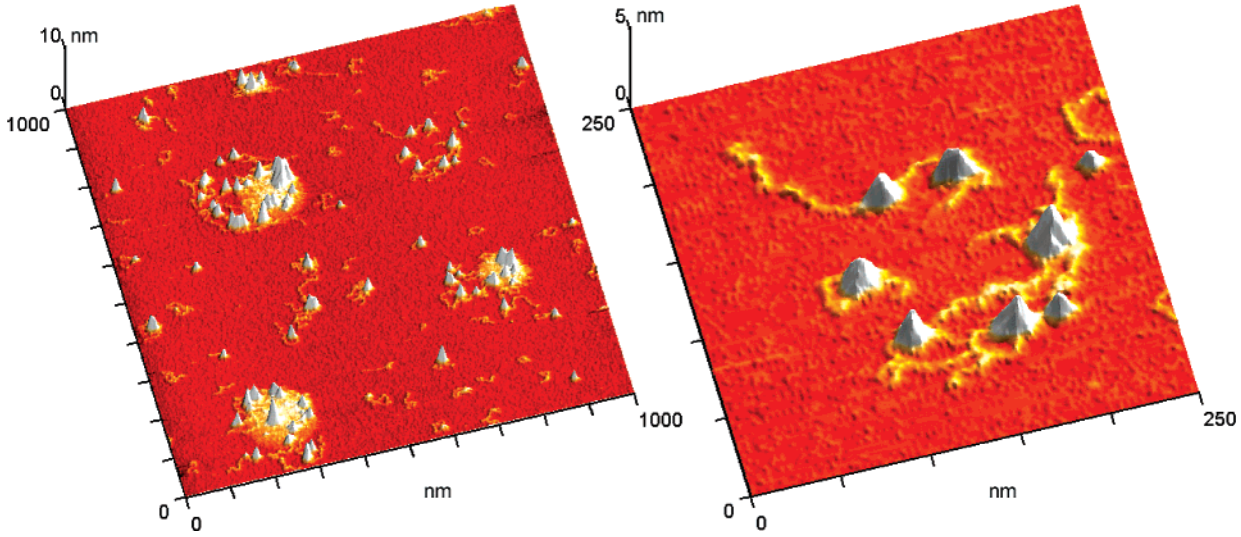

Figure 6. TMAFM images of hybrid nanoparticle−coil copolymer **2** prepared from pBA-*b*-p(S-*r*-BCB) linear precursor **1**. Left: 3-D rendering of 1 μm by 1 μm scan. Right: 250 nm by 250 nm zoomed-in portion of left image. Taller globular features correspond to polystyrenic nanoparticle segments and wormlike threads correspond to individual chains of pBA.

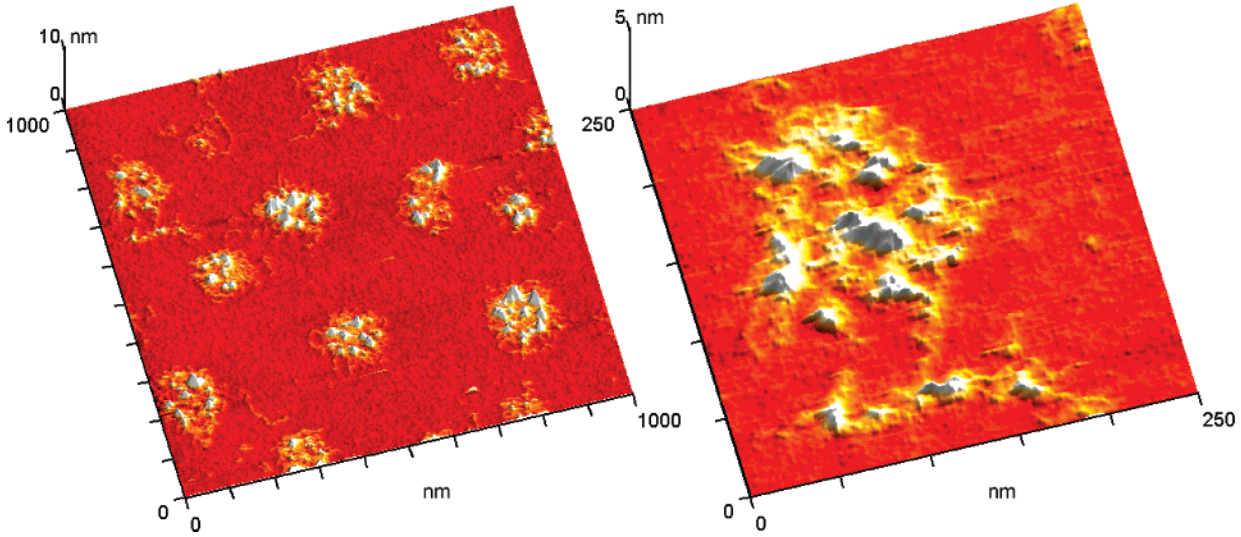

Figure 7. TMAFM images of p(S-*r*-BCB)-*b*-[G-3]-*b*-pBA star copolymers **17**. Copolymers were spin-coated onto a mica surface from a very dilute chloroform solution (5 μg/mL). Left: 3-D rendering of 1 μm by 1 μm scan. Right: 250 nm by 250 nm zoomed-in portion of left image.

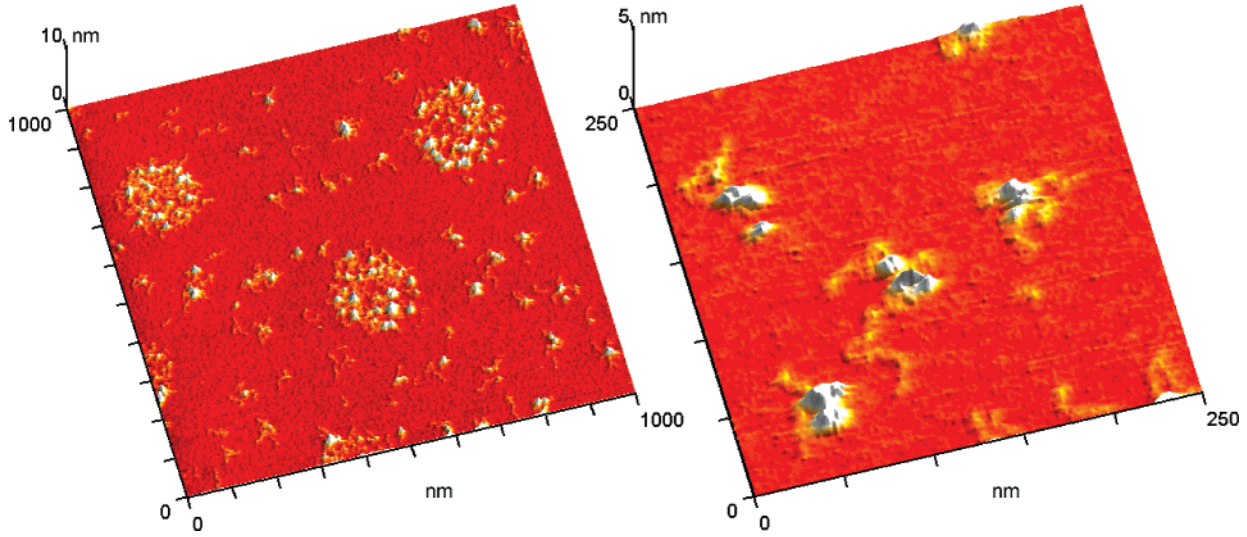

Figure 8. TMAFM images of nanoparticle−coil copolymer **18** prepared from p(S-*r*-BCB)-*b*-[G-3]-*b*-pBA star copolymers **17**. Copolymers were spin-coated onto a mica surface from a very dilute chloroform solution (5 μg/mL). Left: 3-D rendering of 1 μm by 1 μm scan. Right: 250 nm by 250 nm zoomed-in portion of left image.

from the pBA-*b*-p(S-*r*-BCB) linear diblock copolymer precursors were spin-coated onto mica substrates from dilute chloroform solutions (5 μg/mL). By using ultradilute conditions a submonolayer coverage of copolymer chains was obtained which allowed the nanoparticle−coil copolymer **2** to be successfully imaged with high resolution TMAFM (Figure 6). AFM height images revealed the presence of wormlike threads connected to taller globular protrusions. Globular and wormlike features were assigned respectively to 3-dimensional polystyrene nanoparticles and linear pBA segments. Particle-like features were 2−5 nm tall, and their diameter (uncorrected for the finite size of AFM tip) ranged from 10 to 20 nm. This difference indicated that upon deposition on mica, the polystyrene nanoparticles underwent flattening similar to one observed in other similar systems (e.g., shell cross-linked micelles).[24] The overall dimensions of wormlike threads varied, since the linear pBA chains would be expected to adopt both extended and coiled conformations. The composition and architecture of the copolymer was an important factor in facilitating molecular visualization on mica substrates. The presence of the pBA component enabled adsorption and spreading of the linear segment on the surface, while the glassy cross-linked nanoparticle imparted sufficient shape-persistence to allow AFM imaging. Of particular significance was the observation that essentially all nanoparticles had a single pBA chain attached which directly confirms the synthetic methodology.[25] "Particle−coil"-like shapes were not however observed for the corresponding linear pBA-*b*-p(S-*r*-BCB) block copolymers **1**, presumably due to the lack of shape persistence of the polystyrenic block. Instead only globular structures were observed on mica surface for this *linear* block copolymer.

This lack of shape persistence is alleviated to a certain extent in the star copolymer structures due to the 3-dimensionality introduced via the polyether dendrimer. AFM imaging of the star copolymer **17** was therefore performed under similar conditions as for the diblock copolymer, **1**, and the resulting particle−coil copolymer **2** (Figure 7). As with copolymer **2**, particle−coil objects similar to those shown in Figure 6 were discernible, however individual structures were much less resolved and a much higher tendency to form large circular aggregates was observed. The higher tendency of the non-cross-linked star copolymer **17** to form such clusters in comparison with copolymer **2** may be a result of the branched nature of star blocks, which are more likely to be subject to significant entanglement than the compact, cross-linked polystyrenic nanoparticles present in **2**.

A direct comparison with the nanoparticle−coil copolymer **18** prepared from the star copolymer **17** adds further evidence to the importance of macromolecular architecture in these systems. In this case, conversion of the star copolymer to the nanoparticle lead to significantly different behavior and individual molecular species could again be later visualized with TMAFM (Figure 8). Both height and phase images revealed the presence of taller spherical features connected to shorter threadlike extensions corresponding to polystyrenic nanoparticle and pBA coil segments.[24] The apparent lateral size (not corrected for AFM tip size) of particle-like features was in the range of 10−20 nm, and was similar to the size of their counterparts in copolymer **17** (Figure 7). In contrast with un-cross-linked copolymer **17**, a significant fraction of nanoobjects was not associated with large round aggregates. This higher percentage of individual nanoparticle−coil nanoobjects in the AFM images of copolymer **18**, when compared to **17**, points to a reduced aggregation due to cross-linking of the polystyrene block leading to nanoparticle formation.[26]

Conclusion

A novel class of hybrid copolymers, termed nanoparticle−coil copolymers, has been prepared by using a synergistic combination of controlled radical polymerization, benzocyclobutene chain collapse chemistry and convergent dendrimer synthesis. The mixed architecture, nanoparticle−coil copolymers were synthesized from both linear and dendritic precursors, although the use of a dendritic initiator overcame many of the synthetic limitations associated with the linear diblock copolymer approach. Direct visualization of single nanoparticle−coil copolymer architectures was possible using high resolution AFM and the individual elements, globular polystyrene nanoparticle and random coil,

linear poly(butyl acrylate) could be individually observed at molecular resolution. The success at visualizing these materials and their aggregation behavior was found to be directly related to the architecture of the hybrid block copolymer and their ability to undergo entanglement and/or interdigitation. We are currently evaluating these novel hybrids as intelligent nanoporogens for low-*k* dielectric materials, as well-defined building blocks to prepare higher order assemblies, and as biological mimics for therapeutic applications.

Acknowledgment. We thank the MRSEC Program of the National Science Foundation under Award DMR-0213618 for the Center for Polymeric Interfaces and Macromolecular Assemblies, the NIRT Program of the National Science Foundation Grant No. 0210247, IBM Corporation, DOE-BES (LBNL Polymer Program) and AFOSR for financial support.

Supporting Information Available: Text giving the experimental details[27−31] on the synthesis of dendritic initiators, block copolymers, and nanoparticle−coil copolymers. This material is available free of charge via the Internet at http://pubs.acs.org.

References and Notes

(1) (a) Krejchi, M. T.; Atkins, E. D. T.; Waddon, A. J.; Fournier, M. J.; Mason, T. L.; Tirrell, D. A. *Science* **1994**, *265*, 1427. (b) Hartgerink, J. D.; Beniash, E.; Stupp, S. I. *Science* **2001**, *294*, 1684−1688. (c) Amgen's Neulasta is a covalent conjugate of recombinant methionyl human G-CSF, a water-soluble 175 amino acid protein with a MW of approximately 19 000, and monomethoxypoly(ethylene glycol) of MW 20 000. For another example see: Reddy, K.; Wright, T. L.; Pockros, P. J.; Shiffman, M.; Everson, G.; Reindollar, R.; Fired, M. W.; Purdum, P. P.; Jensen, D.; Smith, C.; Lee, W. M.; Boyer, T. D.; Lin, A.; Pedder, S.; DePamphilis, J. *Hepatology* **2001**, *33*, 433−8.

(2) (a) Park, C.; Yoon, J.; Thomas, E. L. *Polymer* **2003**, *44*, 6725−6760. (b) Lodge, T. P. *Macromol. Chem. Phys.* **2003**, *204*, 265. (c) Zubarev, E. R.; Pralle, M. U.; Li, L.; Stupp, S. I. *Science* **1999**, *283*, 523−526. (d) Lee, M.; Cho, B. K.; Zin, W. C. *Chem. Rev.* **2001**, *101*, 3869−3892. (e) Bates, F. S.; Fredrickson, G. H. *Annu. Rev. Phys. Chem.* **1990**, *41*, 32−38. (f) Bates, F. S.; Fredrickson, G. H. *Phys. Today* **1999**, *52*, 32. (g) Hudson, S. D.; Jung, H.-T.; Percec, V.; Cho, W.-D.; Johansson, G.; Ungar, G.; Balagurusamy, V. S. K. *Science* **1997**, *278*, 449−452. (h) Thurmond, K. B.; Kowalewski, T.; Wooley, K. L. *J. Am. Chem. Soc.* **1996**, *118*, 7239. (i) Wooley, K. *J. Polym. Sci., Part A: Polym. Chem.* **2000**, *38*, 1397−1407.

(3) (a) Coates, G. W. *Chem. Rev.* **2000**, *100*, 1223−1252. (b) Buchmeiser, M. R. *Chem. Rev.* **2000**, *100*, 1565−1604. (c) Trnka, T. M.; Grubbs, R. B. *Acc. Chem. Res.* **2001**, *34*, 18−29. (d) Hawker, C. J.; Bosman, A. W.; Harth, E. *Chem. Rev.* **2001**, *101*, 3661−3688. (e) Grayson, S. M.; Fréchet, J. M. J. *Chem. Rev.* **2001**, *101*, 3819−68. (f) Hadjichristidis, N.; Pitsikalis, M.; Pispas, S.; Iatrou, H. *Chem. Rev.* **2001**, *101*, 3747. (g) Matyjaszewski, K.; Xia, J. *Chem. Rev.* **2001**, *101*, 2921−2990. (h) Kamigaito, M.; Ando, T.; Sawamoto, M. *Chem. Rev.* **2001**, *101*, 3689−3745. (i) Hirao, A.; Loykulnant, S.; Ishizone, T. *Prog. Polym. Sci.* **2002**, *27*, 1399−1471. (j) Fréchet, J. M. J. *J. Polym. Sci., Part A: Polym. Chem.* **2003**, *41*, 3713−3725.

(4) (a) Newkome, G. R.; Baker, G. R.; Arai, S.; Saunders, M. J.; Russo, P. S.; Theriot, K. J.; Moorefield, C. N.; Rogers, L. E.; Miller, J. E.; Lieux, T. R.; Murray, M. E.; Phillips, B.; Pascal, L. *J. Am. Chem. Soc.* **1990**, *112*, 8458−8465. (b) Gitsov, I.; Wooley, K. L.; Fréchet, J. M. J. *Angew. Chem., Int. Ed. Engl.* **1992**, *31*, 1200−1202. (c) Chapman, T. M.; Hillyer, G. L.; Mahan, E. J.; Shaffer, K. A. *J. Am. Chem. Soc.* **1994**, *116*, 11195−11196. (d) Vanhest, J. C. M.; Delnoye, D. A. P.; Baars, M. W. P. L.; Vangenderen, M. H. P.; Meijer, E. W. *Science* **1995**, *268*, 1592−1595. (e) Leduc, M. R.; Hawker, C. J.; Dao, J.; Fréchet, J. M. J. *J. Am. Chem. Soc.* **1996**, *118*, 11111−11118. (f) Malenfant, P. R. L.; Groenendaal, L.; Fréchet, J. M. J. *J. Am. Chem. Soc.* **1998**, *120*, 10990−10991. (g) Iyer, J.; Fleming, K.; Hammond, P. T. *Macromolecules* **1998**, *31*, 8757−8765. (h) Zubarev, E. R.; Pralle, M. U.; Sone, E. D.; Stupp, S. I. *J. Am. Chem. Soc.* **2001**, *123*, 4105−4106. (i) Zubarev, E. R.; Stupp, S. I. *J. Am. Chem. Soc.* **2002**, *124*, 5762−5773. (h) Johnson, M. A.; Iyer, J.; Hammond, P. T. *Macromolecules* **2004**, *37*, 2490−2501.

(5) (a) Mackay, M. E.; Hong, Y.; Jeong, M.; Tande, B. M.; Wagner, N.; Hong, S.; Gido, S. P.; Vestberg, R.; Hawker, C. J. *Macromolecules* **2002**, *35*, 8391. (b) Pochan, D. J.; Pakstis, L.; Huang, E.; Hawker, C. J.; Vestberg, R.; Pople, J. *Macromolecules* **2002**, *35*, 9239−9242.

(6) Ihre, H. R.; Padilla De Jesús, O.; Szoka, F. C., Jr.; Fréchet, J. M. J. *Bioconj. Chem.* **2002**, *13*, 443−52.

(7) (a) Hadjichristidis, N.; Pitsikalis, M.; Pispas, S.; Iatrou, H. *Chem. Rev.* **2001**, *101*, 3747. (b) Pitsikalis, M.; Pispas, S.; Mays, J. W.; Hadjichristidis, N. *Adv. Polym. Sci.* **1998**, *135*, 1−137. (c) Roovers, J.; Comanita, B. *Adv. Polym. Sci.* **1999**, *142*, 179−228. (d) Al-Muallem, H. A.; Knauss, D. M. *J. Polym. Sci., Polym. Chem.* **2001**, *39*, 152−161.

(8) Harth, E.; Van Horn, B.; Lee, Y. V.; Germack, D. S.; Gonzales, C. P.; Miller, R. D.; Hawker, C. J. *J. Am. Chem. Soc.* **2002**, *124*, 8653−8660.

(9) (a) Hansma, H. G.; Vesenka, J.; Kelderman, G.; Morrett, H.; Sinsheimer, R. L.; Elings, V.; Bustamante, C.; Hansma, P. K. *Science* **1992**, *256*, 1180. (b) Tsukruk, V.; Reneker, D. H. *Polymer* **1995**, *36*, 1791−1808. (c) Magonov, S. N.; Reneker, D. H. *Annu. Rev. Mater. Sci.* **1997**, *27*, 175−222. (d) Sheiko, S. S. *Adv. Polym. Sci.* **2000**, *151*, 61−174. (e) Sheiko, S. S.; Möller, M. *Chem. Rev.* **2001**, *101*, 4099−4123. (f) Kumaki, J.; Hasimoto, T. *J. Am. Chem. Soc.* **2003**, *125*, 4907−4917. (g) Kiriy, A.; Gorodyska, G.; Minko, S.; Tsitsilianis, C.; Jaeger, W.; Stamm, M. *J. Am. Chem. Soc.* **2003**, *125*, 11202−11203.

(10) (a) Li, J.; Swanson, D. R.; Qin, D.; Brothers, H. M.; Piehler, L. T.; Tomalia, D.; Meier, D. J. *Langmuir* **1999**, *15*, 7347−7350. (b) Zhang, H.; Grim, P. C. M.; Foubert, P.; Vosch, T.; Vanoppen, P.; Wiesler, U. M.; Berresheim, A. J.; Müllen, K.; DeSchryver, F. C. *Langmuir* **2000**, *16*, 9009−9014. (c) Li, J.; Piehler, L. T.; Qin, D.; Baker, J. R.; Tomalia, D. A.; Meier, D. J. *Langmuir* **2000**, *16*, 5613. (d) Li, J.; Qin, D. J.; Baker, J. R.; Tomalia, D. A. *Macromol. Symp.* **2001**, *167*, 257−269. (e) Takada, K.; Diaz, D. J.; Aburna, H. D.; Cuadrado, I.; Gonzales, B.; Casado, C. M.; Alonso, B.; Moran, M.; Losada, J. *Chem.−Eur. J.* **2001**, *7*, 1109−1117. (f) Betley, T. A.; Hessler, J. A.; Mecke, A.; Banazak Holl, M. M.; Orr, B. G.; Uppuluri, S.; Tomalia, D. A.; Baker, J. R. *Langmuir* **2002**, *18*, 3127−3133. (g) Ruiz, J.; Lafuente, G.; Marcen, S.; Ornelas, C.; Lazare, S.; Cloutet, E.; Blais, J. C.; Astruc, D. *J. Am. Chem. Soc.* **2003**, *125*, 7250−7257. (f) Choi, Y.; Mecke, A.; Bradford, G. O.; Banazak Holl, M. M.; Baker, J. R. *Nano Lett.* **2004**, *4*, 391−397.

(11) (a) Sheiko, S. S.; Gauthier, M.; Möller, M. *Macromolecules* **1997**, *30*, 2343. (b) Kiriy, A.; Gorodyska, G.; Minko, S.; Tsitsilianis, C.; Stamm, M. *Macromolecules* **2003**, *36*, 8704−8711. (d) Pyun, J.; Kowalewski, T.; Matyjaszewski, K. *Macromol. Rapid Commun.* **2003**, *24*, 1043−1059. (e) Li, J.; Gauthier, M.; Teertstra, S. J.; Xu, H.; Sheiko, S. S. *Macromolecules* **2004**, *37*, 795−802. (f) Schappacher, M.; Deffieux, A.; Putaux, J. L.; Viville, P.; Lazzaroni, R. *Macromolecules* **2003**, *36*, 5776−5783.

(12) (a) Percec, V.; Ahn, C. H.; Ungar, C. H.; Yeardley, D. J. P.; Moeller, M.; Sheiko, S. S. *Nature (London)* **1998**, *391*, 161−164. (b) Percec, V.; Ahn, C.-H.; Cho, W.-D.; Jamieson, A. M.; Kim, J.; Leman, T.; Schmidt, M.; Gerle, M.; Möller, M.; Prokhorova, S. A.; Sheiko, S. S.; Cheng, S. Z. D.; Zhang, A.; Ungar, G.; Yeardley, D. J. P. *J. Am. Chem. Soc.* **1998**, *120*, 8619−8631. (c) Prokhorova, S. A.; Sheiko, S. S.; Möller, M.; Ahn, C.-H.; Percec, V. *Macromol. Rapid Commun.* **1998**, *19*, 359. (d) Shulter, A. D.; Rabe, J. R. *Angew. Chem., Int. Ed.* **2000**, *39*, 864−883. (e) Shu, L.; Schäfer, A.; Schlüter, A. D. *Macromolecules* **2000**, *33*, 4321−4328. (f) Grayson, S. M.; Fréchet, J. M. J. *Macromolecules* **2001**, *34*, 6542−44. (g) Shu, L.; Schlüter, A. D.; Ecker, C.; Severin, N.; Rabe, J. P. *Angew. Chem., Int. Ed. Engl.* **2001**, *113*, 4666−4669. (h) Zhang, A.; Vetter, S.; Schlüter, A. D. *Macromol. Chem. Phys.* **2001**, *202*, 3301−3315. (i) Shu, L.; Gössl, I.; Rabe, J. P.; Schlüter, A. D. *Macromol. Chem. Phys.*. **2002**, *203*, 2540−2550. (j) Zhang, A.; Zhang, B, Wächtersbach, E.; Schmidt, M.; Schlüter, A. D. *Chem.−Eur. J.* **2003**, *9*, 6083−6092. (k) Liang, C. O.; Helms, B.; Hawker, C. J.; Fréchet, J. M. J. *Chem. Commun.* **2003**, 2524−2525. (l) Zhang, A.; Shu, L.; Bo, Z.; Schlüter, A. D. *Macromol. Chem. Phys.* **2003**, *204*, 328−339. (m) Ecker, C.; Shu, L.; Schlüter, A. D.; Rabe, J. P. *Macromolecules* **2004**, *37*, 2484−2489.

(13) (a) Sheiko, S. S.; Gerle, M.; Fischer, K.; Schmidt, M.; Möller, M. *Langmuir* **1997**, *13*, 5368−5372. (b) Beers, K. L.; Gaynor, S. G.; Matyjaszewksi, K.; Sheiko, S. S.; Möller, M. *Macromolecules* **1998**, *31*, 9413. (c) Djalali, R.; Hugenberg, N.; Fischer, K.; Schmidt, M. *Macromol. Rapid Commun.* **1999**, *20*, 444−449. (d) Gerle, M.; Fischer, K.; Roos, S.; Muller, A. H. E.; Schmidt, M.; Sheiko, S. S.; Prokhorova, S.; Möller, M. *Macromolecules* **1999**, *32*, 2629−2637. (e) Boerner, H. G.; Beers, K. L.; Matyjaszewski, K.; Sheiko, S. S.; Möller, M. *Macromolecules* **2001**, *34*, 4375. (f) Cheng, G.; Boeker, A.; Zhang, M.; Krausch, G.; Mueller, A. H. E. *Macromolecules* **2001**, *34*, 6883. (g) Sheiko, S. S.; Prokhorova, S. A.; Beers, K. L.; Matyjaszewski, K.; Potemin, I. I.; Khokhlov, A. R.; Moeller, M. *Macromolecules* **2001**, *34*, 8354. (h) Fischer, K.; Schmidt, M. *Macromol. Rapid Commun.* **2001**, *22*, 787−791. (i) Djalali, R.; Li, S.-Y.; Schmidt, M. *Macromolecules* **2002**, *35*, 4282. (j) Boerner, H. G.; Duran, D.; Matyjaszewski, K.; da Silva, M.; Sheiko, S. S. *Macromolecules* **2002**, *35*, 3387−3394. (k) Matyjaszewski, K.; Qin, S.; Boyce, J. R.; Shirvanyants, D.; Sheiko, S. S. *Macromolecules* **2003**, *125*, 1843. (l) Neugebauer, D.; Zhang, Y.; Pakula, T.; Sheiko, S. S.; Matyjaszewski, K. *Macromolecules* **2003**, *36*, 6746−6755. (m) Sheiko, S. S.; da Silva, M.; Shirvaniants, D. G.; Larue, I.; Prokhorova, S. A.; Möller, M.; Beers, K. L.; Matyjaszewksi, K. *J. Am. Chem. Soc.* **2003**, *125*, 6725. (n) Zhang, M. F.; Breiner, T.; Mori, H.; Muller, A. H. E. *Polymer* **2003**, *44*, 1449−1458. (o) Lord, S. J.; Sheiko, S. S.; LaRue, I.; Lee, H. I.; Matyjaszweski, K. *Macromolecules* **2004**, *37*, 4235−4240. (p) Zhang, M. F.; Drechsler, M.; Muller, A. H. E. *Chem. Mater.* **2004**, *16*, 537−543.

(14) Boyce, J. R.; Shirvanyants, D.; Sheiko, S. S.; Ivanov, D. A.; Qin, S.; Borner, H.; Matyjaszewski, K. *Langmuir* **2004**, *20*, 6005−6011.

(15) Prokhorova, S. A.; Sheiko, S. S.; Mourran, A.; Azumi, A.; Beginn, U.; Zipp, G.; Ahn, C.-H.; Holerca, N. M.; Percec, V.; Möller, M. *Langmuir* **2000**, *16*, 6862−6867.

(16) Barner, J.; Mallwitz, F.; Shu, L.; Schlüter, A. D.; Rabe, J. P. *Angew. Chem., Int. Ed. Engl.* **2003**, *42*, 1932.

(17) (a) Benoit, D.; Chaplinski, V.; Braslau, R.; Hawker, C. J. *J. Am. Chem. Soc.* **1999**, *121*, 3904−3920. (b) Blomberg, S.; Ostberg, S.; Harth, E.; Bosman, A. W.; Van Horn, B.; Hawker, C. J. *J. Polym. Sci., Part A: Polym. Chem.* **2002**, *40*, 1309−1320.

(18) (a) Gómez Ribelles, J. L.; Meseguer Dueñas, J. M.; Torregrosa Cabanilles, C.; Monleón Pradas, M. *J. Phys.: Condens. Matter* **2003**, *15*, S1149−S1161. (b) Widmaier, J. M.; Sperling, L. H. *Macromolecules* **1982**, *15*, 625−631.

(19) Hawker, C. J.; Fréchet, J. M. J. *J. Am. Chem. Soc.* **1990**, *112*, 7638.

(20) Pyun, J.; Rees, I.; Fréchet, J. M. J.; Hawker, C. J. *Aust. J. Chem.* **2003**, *56*, 775−782.

(21) (a) Matyjaszewski, K.; Miller, P. J.; Pyun, J.; Kickelbick, G.; Diamanti, S. *Macromolecules* **1999**, *32*, 6526−6535. (b) Angot, S.; Murthy, K. S.; Taton, D.; Gnanou, Y. *Macromolecules* **1998**, *31*, 7218−7225. (c) Angot, S.; Murthy, K. S.; Taton, D.; Gnanou, Y. *Macromolecules* **2000**, *33*, 7261−7274.

(22) *N*,*N*′,*N*′,*N*″-Pentamethyldiethylenetriamine (PMDETA) was used as the ligand in these experiments. General optimization of ATRP using the $Cu^{I}Br$/PMDETA catalyst system and other reactive catalysts are described in the following references: (a) Xia, J.; Matyjaszewski, K. *Macromolecules* **1997**, *30*, 7697−7700. (b) Xia, J.; Gaynor, S. G.; Matyjaszewski, K. *Macromolecules* **1998**, *31*, 5958−5959. (c) Queffelec, J.; Gaynor, S. G.; Matyjaszewski, K. *Macromolecules* **2000**, *33*, 8629−8639.

(23) The initiation efficiency is calculated by the ratio of the $M_{n\ theoretical}$ vs $M_{n\ experimental}$, where $M_{n\ theoretical}$ is defined as $\Delta[M]/[I]_o \times MW_{monomer}$, and $M_{n\ experimental}$ values were determined from SEC and ^1H NMR.

(24) (a) Murthy, K. S.; Ma, Q.; Remsen, E. E.; Kowalewski, T.; Wooley, K. L. *J. Mater. Chem.* **2003**, *13*, 2785−2795. (b) Huang, H. Y.; Kowalewski, T.; Wooley, K. L. *J. Polym. Sci., Part A: Polym. Chem.* **2003**, *41*, 1659−1668.

(25) A limited number of "free" poly(butyl acrylate) chains were observed in AFM images of the hybrid nanoparticle−coil systems. These may be attributed to an artifact of the spinning process due to potential cleavage of the polystyrene nanoparticle from the block copolymer under the very high shear forces present during deposition.

(26) Single-molecule visualization of the reverse (PBA−nanoparticle)−(PSt−coil) copolymer **22** using AFM was significantly more challenging than for **2** and **18**, as the composition of the copolymer were not ideally suited for imaging on a mica surface. AFM imaging of **22** under various conditions (e.g., on graphite substrates) is the subject of ongoing studies.

(27) Matyjaszewski, K.; Patten, T. E.; Xia, J. *J. Am. Chem. Soc.* **1997**, *119*, 674−680.

(28) (a) Benoit, D.; Chaplinski, V.; Braslau, R.; Hawker, C. J. *J. Am. Chem. Soc.* **1999**, *121*, 3904−3920. (b) Blomberg, S.; Ostberg, S.; Harth, E.; Bosman, A. W.; Van Horn, B.; Hawker, C. J. *J. Polym. Sci., Part A: Polym. Chem.* **2002**, *40*, 1309−1320.

(29) Harth, E.; Van Horn, B.; Lee, Y. V.; Germack, D. S.; Gonzales, C. P.; Miller, R. D.; Hawker, C. J. *J. Am. Chem. Soc.* **2002**, *124*, 8653−8660.

(30) Pyun, J.; Rees, I.; Fréchet, J. M. J.; Hawker, C. J. *Aust. J. Chem.* **2003**, *56*, 775−782.

(31) Mackay, M. E.; Hong, Y.; Jeong, M.; Tande, B. M.; Wagner, N.; Hong, S.; Gido, S. P.; Vestberg, R.; Hawker, C. J. *Macromolecules* **2002**, *35*, 8391.

MA047375F